Asian Journal of Chemistry; Vol. 28, No. 10 (2016), 2292-2298

ASIAN JOURNAL OF CHEMISTRY

http://dx.doi.org/10.14233/ajchem.2016.19972

Electrochemical Properties of Co Films by Electrolytic Deposition

CHANG-SUK HAN[1,*] and TAE-SOO JANG[2]

[1]Department of Defense Science & Technology, Hoseo University, Hoseo-ro 79beon-gil, Baebang-Myun, Asan City, Chungnam 31499, Republic of Korea
[2]Department of Nanobiotronics, Hoseo University, Hoseo-ro 79beon-gil, Baebang-Myun, Asan City, Chungnam 31499, Republic of Korea

*Corresponding author: Tel: +82 41 5409542; E-mail: hancs@hoseo.edu

Received: 14 March 2016; *Accepted*: 10 June 2016; *Published online*: 30 June 2016; AJC-17984

Both electroless-deposited CoP and CoFeB films and electro-deposited Co films are formed on rapid-quenched amorphous alloy ribbons. These polycrystalline Co-based films were obtained with different preferred orientations, surface structures and magnetic properties, from the species of substrates. Electrochemical characterizations by means of polarization curve clarified the catalytic activity of electrodes and the over potential, for electroless- and electro-depositions, respectively. These electrochemical properties may affect the first stage of deposition, to determine the structural and magnetic properties of the films. It is found that the structural and magnetic properties of non-electrically deposited films are determined by the initial step of electrochemical parameters dependent on the species of substrate. This is because the nucleation and crystal growth are related to electrocatalysis of substrate electrode for anodic oxidation of the reductant in non-electric deposition and over-potential of electrodeposition, whose parameters are dependent on the alloy element of substrate. The properties of both non-electrically deposited and electrically deposited films of a few micrometers thick are influenced by the initial behaviour of electrolytic deposition.

Keywords: Electroless-deposition, Amorphous alloy ribbon, Co-based film, Magnetic property, Electrochemical characterization.

INTRODUCTION

Both rapid-quenching amorphous ribbon and electrolytic-deposited film are well known as low-cost materials prepared from liquid phase [1-6]. To our best of knowledge, there has been a little research on the bimetal material of electrolytic films deposited on ribbon. Our investigation of this bimetal material was mainly focused on how interface stress, which was induced by crystallization of amorphous ribbon during annealing of the bimetal, affected magnetic properties of the film layer. On the other hand, a fundamental characterization of electrolytic deposition behaviour and the structural and magnetic properties of the film layer have been performed [7].

It is known that Co-Fe alloy exhibits increased saturation magnetization (M_s) and positive transition of negative saturation magnetostriction (λ_s), with increasing Fe content. Therefore, the alloy enriched with Fe content is raising expectations as a soft magnetic material with a large M_s (larger than that of permalloy) and as a new material with M_s and large L_s. However, there has been little work with respect to electrochemical deposition, because of the technical problems of Fe deposition from an aqueous solution. non-electrical deposition proceeds by metal ion reduction accompanied by anodic oxidation of the reducing agent in an electrolyte, while electrodeposition proceeds under an applied cathodic current. In the case of an electrolyte containing P (or B) and S as a complexing agent or a reductant, the metalloid element also deposits, forming an alloy-metalloid phase. Cavallotti *et al.* [8] showed that Co-Fe alloy deposits with a wide range of composition were obtainable on nickel-based amorphous alloy ribbons, by selecting the electrolytic conditions. Furthermore, they found that the structural and magnetic properties of non-electrically deposited Co-P alloys (a few micrometers in thickness) were dependent on the alloying element of amorphous ribbons [9]. It is generally known that the properties of such thick deposits are obtained independently of substrate species.

In this paper, the electrochemical behaviour and the structural and magnetic properties of non-electrically deposited Co-P and Co-Fe-B and electrodeposited Co were investigated in terms of substrate species: Ni-, Co- and Fe-based amorphous alloys and polycrystalline copper.

EXPERIMENTAL

Non-electric deposition and electrodeposition were carried out on an electrode (substrate) in an isothermal electrolytic

cell (300 mL in volume). Table-1 shows the compositions of the electrolyte and electrolytic conditions.

TABLE-1
COMPOSITION OF NON-ELECTRICAL CoP DEPOSITION BATH (A), NON-ELECTRICAL CoFe DEPOSITION BATH (B) AND ELECTRODEPOSITION BATH OF Co (C) AND THEIR DEPOSITION CONDITIONS

Chemicals	A; E.L. CoP	B; E.L. CoFeB	C; E. Co
Na-citrate	0.2	0.20	–
$CoSO_4 \cdot 7H_2O$	0.1	0.04	0.5
$(NH_4)_2Fe(SO_4)_2$	–	0.01	–
$NaH_2PO_2 \cdot H_2O$	0.2	–	–
Dimethylaminoborane	–	0.025	–
H_3BO_3	0.5	–	–
pH	8.2	10	5.0
pH of adjustment	NaOH soln.	NH_4OH soln.	H_2SO_4 soln.
Bath temp. (°C)	85	85	30

Table-2 shows the compositions of the amorphous alloys (prepared by the single-roll method), which exhibited non-crystalline phase analyzed by X-ray diffractometry. Polycrystalline copper sheet (purity 99.9 %, thickness 0.5 mm) was a commercial product.

TABLE-2
COMPOSITION OF RAPID-QUENCHED AMORPHOUS ALLOY RIBBONS USED AS SUBSTRATES

Species	Composition (at %)
Sample N	$Ni_{76}Si_4B_{20}$
Sample F	$Fe_{84}Si_1B_{15}$
Sample C	$Co_{69}Fe_4Si_{16}B_9Mo_2$

Substrate electrodes of 10×10 mm^2 surface area for non-electric deposition were used as a cathode after chemical polishing by rinsing in 10 % HCl and 10 % HF solutions for 30 min, in the case of Fe- and Co-based substrates and Ni-based and copper ones, respectively, followed by sensitizing and catalyzing. The sensitizing and catalyzing solutions were 40 g/L $SnCl_2 \cdot 2H_2O$ + 20 mL/L HCl for 2 min and 0.3 g/L $PdCl_2 \cdot 2H_2O$ + 5 mL/L HCl for 1 min. On the other hand, electrodeposition was carried out is galvanostatic mode, after mechanical polishing with emery paper up to # 1500 followed by ultrasonic rinsing. The electrochemical polarization measurement was made in potential sweep mode (potential sweep rate 1 mV/s). The working electrode was a substrate treated under the same conditions as for deposition, the counter electrode a spiral platinum wire and the reference electrode is a saturated silver electrode (SSE). For the non-electrodeposition bath, which was designated as the total bath, an anodic and a cathodic polarization curve (i-E curve) was measured. The anodic and cathodic i-E curves were obtained for a solution without metal ions, the anodic partial bath and one without a reducing agent, the cathodic partial bath. On the other hand, only cathodic i-E curve was measured for the electrodeposition bath. The film thickness was calculated from mass gain during deposition using the density of Co and Co-Fe alloy. Composition of deposits were analyzed by atomic absorbance method. The current efficiency was estimated by mass gain and electric charge passed. Surface morphology of the deposit was observed by scanning electron microscopy (SEM; JSM-890S JEOL) and the magnetic properties were estimated by vibrating sample magnetometer (VSM; VSM 5-15 TOEI Indus. Co.). The characterization of crystalline preferred orientation was obtained by X-ray diffractometer (XRD; JDX-35HS JEOL). The "degree of preferred orientation" was defined as the ratio of each peak intensity ratio obtained to that listed on JCPDS card.

RESULTS AND DISCUSSION

Non-electrical Co and Co-Fe alloy deposition: The Co-P, Co-B and Co-Fe-B were non-electrically deposited on amorphous ribbons from an electrolyte containing sodium hypophosphite monohydrate (NaH_2PO_3-H_2O) or dimethylaminoborane (DMAB) as a reducing agent. Since there have been reports on the electrochemical polarization behaviour of Co-B and Co-Fe-B deposition and the structural and magnetic properties of Co-Fe-B deposits, we will discuss the influence of alloying composition on electrochemical parameters and structural properties below [7].

Non-electrical deposition from electrolyte Containing $NaH_2PO_3 \cdot H_2O$: Fig. 1 shows the XRD profiles of non-electrically deposited Co-P on the roll side surface of Fe- and Ni-based amorphous ribbons and polycrystalline Cu sheet, where the deposits are (a) on non-catalyzed Fe-based alloy (Sample F), (b) on catalyzed Fe-based alloy (Sample F), (c) on catalyzed Cu and (d) on catalyzed Ni-based alloy (Sample N). The film thickness of deposits is shown on the right side of Fig. 1. Each thickness value was obtained after deposition for 1 h. The deposit was not obtained on non-catalyzed Ni-based ribbon. Except for profile (d), the profiles contained the diffraction peaks of hop Co, (1100), (002) and (101) in the deposits. Profile (d) exhibited only the (002) peak. Profiles (c) and (d) revealed diffraction from the substrate, two sharp peaks of fcc Cu and broad peak of amorphous, respectively. It is clear that crystalline preferred orientation of deposits were different from the alloying element of the substrate. A large intensity of (100) was obtained for non-catalyzed iron-based amorphous ribbon substrate [profile (a)] and broad Co peak for the other catalyzed substrates (the other profiles). Comparing among these profiles [(b) to (d)], the preferred orientation of deposits may be dependent even on alloying element of the catalyzed substrate. Surface morphology of deposits was also dependent on the alloying elements of substrates [7].

In non-electrical deposition, the cathodic reduction of metal ions to adsorbed atoms is the initial step, followed by nucleation and crystal growth processes. Therefore, the difference of such deposit thickness as shown in Fig. 1 cannot be explained by autocatalytic reaction of Co-P deposition on the Co-P electrode (deposit surface), which is characterized by conventional polarization measurement. Our image is that the initial step of deposition is familiar to the reaction on substrate surface whose electrode potential is different from that of the deposit surface. We believe that this potential is determined by electrocatalysis of substrate surface, which is designated as the electrocatalysis of the substrate electrode. In order to reveal this initial deposition, the electrochemical polarization (i-E) curves were measured using the substrate

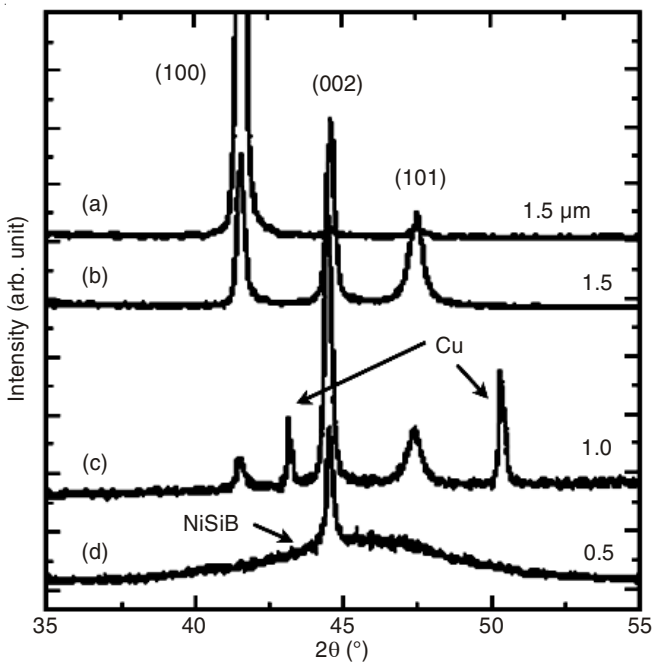

Fig. 1. XRD profiles of non-electrically deposited CoP films on respective amorphous and Cu substrates. (a) non-catalyzed FeSiB (F) ribbon; (b) catalyzed FeSiB (F) ribbon; (c) catalyzed polycrystalline Cu sheet; (d) catalyzed NiSiB (N) ribbon

immersed as the working electrode. Then, the deposition potential and the rate of non-electric deposition are evaluated from anodic and cathodic polarization curves by the conventional method.

Fig. 2(a) and (b) show the total (a) and the partial cathodic and anodic i-E curves (b) for non-electric Co-P deposition on Fe- and Ni-based alloy ribbons, where the data for non-catalyzed and catalyzed amorphous alloys are shown as dotted and solid lines, respectively. In the partial bath, an intersection existed between the anodic and cathodic i-E curves. In the total bath, the deposition rate and the deposition potential were evaluated by extrapolating from two i-E curves and magnitude of deposition rate above about 0.5 mA/cm^2 was obtained, except for non-catalyzed Ni-based electrode. This means that whether non-electric deposition has occurred is determined by the deposition rate on the substrate surface in the initial step [7]. In practice, the non-electric Co-P deposit was not obtainable on non-catalyzed Ni-based amorphous ribbon and Cu sheet.

It is well known that electro catalysis for the anodic oxidation of reductant can be characterized by the potential of anodic partial curve at a current density of 0.1 mA/cm^2, which is designated as the anodic oxidation potential [6]. It is suggested that the electrocatalysis of amorphous ribbon is characterized from the polarization curves as shown in Fig. 2. At first, for the non-catalyzed electrodes, Fig. 2(a) shows that electrocatalysis of Ni-based amorphous electrode is larger than that of Fe-based amorphous one for anodic oxidation of $NaH_2PO_3 \cdot H_2O$. The amount of anodic current whose slope saturates (the limited current) for Ni-based amorphous electrode is smaller than that for the Fe-based amorphous electrode. This is due to the difference of Tafel slope of the anodic current, because of the potential of Fe-based amorphous electrode at which the anodic current saturates similar to that of Ni-based

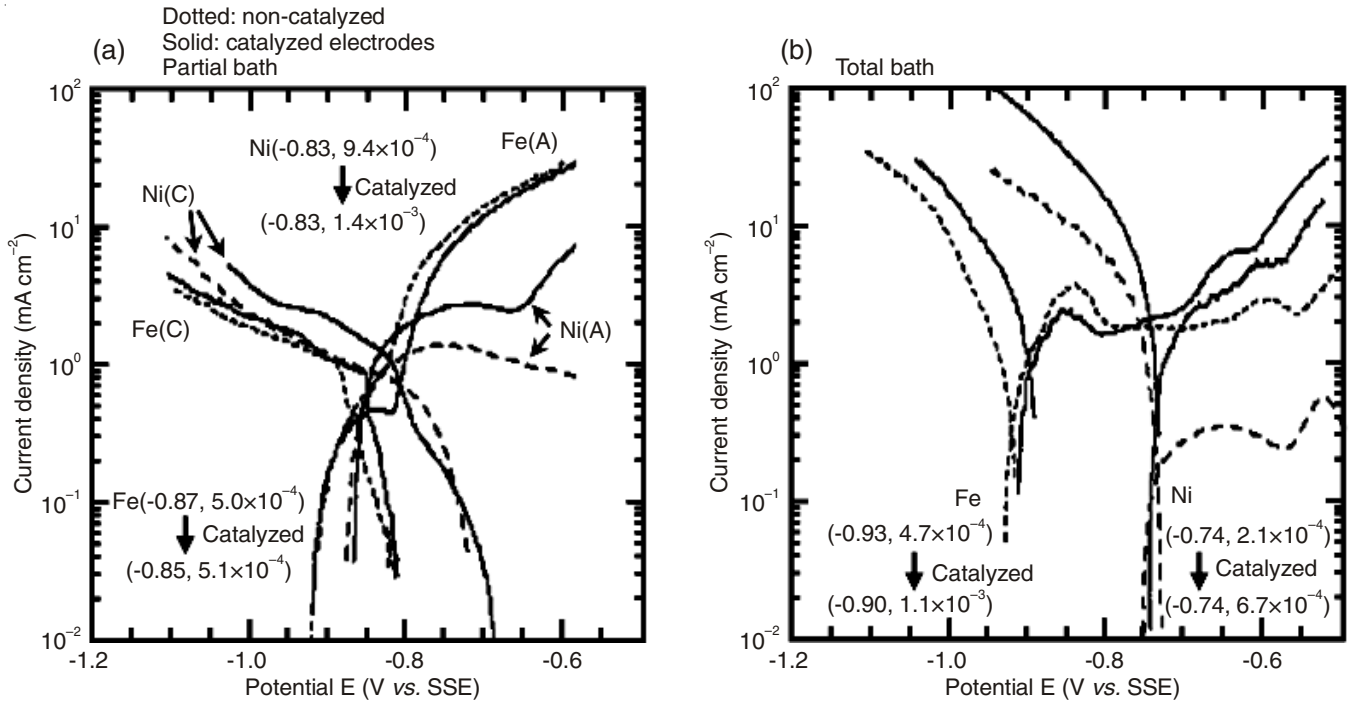

Fig. 2. Electrochemical polarization curves of amorphous FeSiB (S) and NiSiB (N) ribbon electrodes. These curves are described as the thin and thick curves, respectively. (a) In the partial bath, E_{p1} = -0.87 (V *versus* SSE) and i_{p1} = 0.50 (mA/cm^2) for the non-catalyzed FeSiB electrode and E_{p1} = -0.85 and i_{p1} = 0.51 for the catalyzed one. On the other hand, E_{p1} = -0.83 and i_{p1} = 0.94 for the non-catalyzed NiSiB electrode and E_{p1} = -0.83 and i_{p1} = 1.4 for the catalyzed one. (b) In the total bath, E_{p1} = -0.93 and i_{p1} = 0.47 for the non-catalyzed FeSiB electrode and E_{p1} = -0.90 and i_{p1} = 1.1 for the catalyzed one. On the other hand, E_{p1} = -0.74 and i_{p1} = 0.21 for the non-catalyzed NiSiB electrode and E_{p1} = -0.74 and i_{p1} = 0.67 for the catalyzed one. Solid and dotted curves indicate those of catalyzed and non-catalyzed electrodes, respectively

one. Such polarization behaviour was consistent with the fact that Co-P was deposited on Ni-based amorphous electrode but on Fe-based one. Secondly, we will discuss the effect of catalyzing treatment of these amorphous electrodes on electrocatalysis. The anodic oxidation potential of each catalyzed electrode was smaller than that of each non-catalyzed one. This result was explained by anodic oxidation potential of the Pd electrode being less noble than that of the Fe-based and Ni-based amorphous electrode, which was consistent with the investigation of electrocatalysis for the electrodeposited Pd, Ni, *etc.* [4]. For the Ni-based amorphous electrode, the amount of limited current was significantly increased by catalyzing treatment. This means that Tafel slope of the anodic current of Ni-based amorphous electrode was larger than that of the Fe-based one. It is believed that electrocatalysis was determined not only by anodic oxidation potential but also by Tafel slope of anodic current. Therefore, the deposit was obtained on the catalyzed electrode rather than on the non-catalyzed Ni-based amorphous electrode. The experiment revealed that deposit thickness was related to electrocatalysis of the substrate electrode, so that this electrocatalysis may be effective even with a thickness of micrometer order.

Non-electrical deposition from electrolyte containing DMAB: It is possible to deposit non-electrically, Co-B and Co-Fe-B on non-catalyzed Ni-based amorphous ribbon in an electrolyte, using DMAB as a reducing agent. We have described the details of deposition behaviour before [7] and here we focus on the effect of catalyzing treatment of amorphous ribbon surface on non-electric Co-Fe-B alloy deposition. We will present the anomalous deposition behaviour in terms of electrocatalysis of the substrate electrode.

Non-electrical deposition was carried out on the roll side surface of Ni-based ribbon, which was catalyst-treated several times for 0 to 60 s after Sn-sensitizing for 60 s. The deposits exhibited coexistence of bcc Fe and fcc Co (or hcp Co, which is not distinguishable by XRD alone) phases, each of which was a solid solution. XRD profiles of these deposits (Fig. 3) explains the ratio of two phases of the deposit *versus* the duration of catalyzing treatment. In order to evaluate the influence of catalyzing treatment on electrocatalysis of amorphous ribbon electrode for anodic oxidation of DMAB, the anodic i-E curves were measured in the anodic partial bath.

Fig. 4 shows i-E curves for several amorphous electrodes of the roll side of ribbons and the catalyzed Cu sheet. Even the electrocatalysis of non-catalyzed ribbon electrodes exceeded that of the catalyzed copper substrate. The effect of catalyzing treatment on electrocatalysis of amorphous ribbon electrode consisted of a shift of the anodic oxidation potential in a more favourable direction and a decrease in the gradient of anodic oxidation current, behaviour similar to that when using $NaH_2PO_3 \cdot H_2O$ as a reducing agent. It is speculated that area density of Pd on the substrate surface is dependent on the duration of catalyzing treatment, which results in an influence on electrocatalysis of the substrate electrode. It is suggested that crystallinity of the deposits shown in Fig. 3 is caused by the initial step of electrochemical deposition behaviour with the deposition potential determined by electrocatalysis of the substrate electrode.

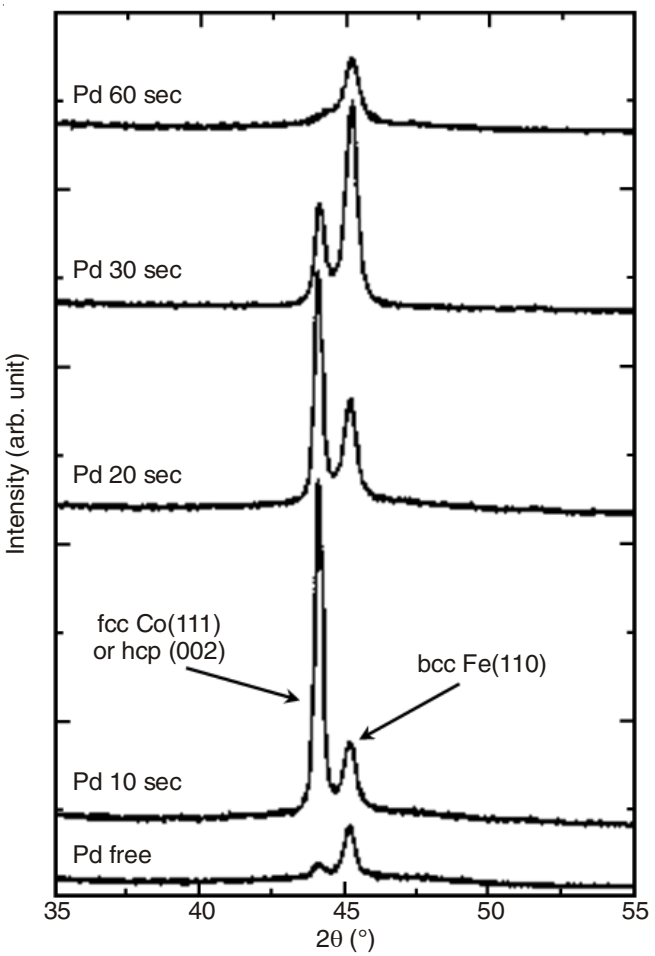

Fig. 3. XRD profiles of non-electrically deposited Co-Fe-B films on amorphous NiSiB (N) ribbon electrodes. The dependences of the crystal phase of films on the time of catalyzing treatment

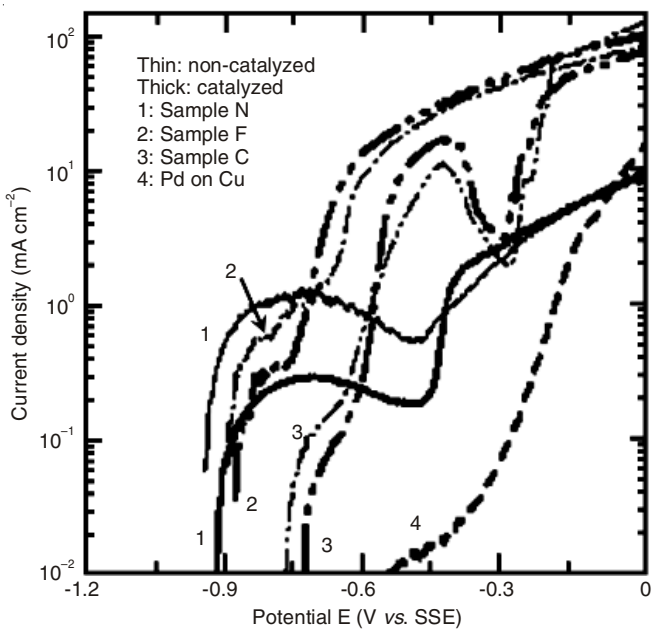

Fig. 4. Partial anodic polarization curves of respective amorphous ribbons, in the partial bath containing Na-citrate and DMAB as a reducing agent. Regular and bold curves refer to non-catalyzed and catalyzed electrodes, respectively

The electrochemical behaviour of non-electric deposition is summarized as follows: The initial step of non-electric deposition is evaluated by electrochemical polarization measurement using the substrate as an electrode, where the deposition potential is influenced by electrocatalysis of the substrate electrode, dependent on the alloying element of the substrate and is caused by the change in electrocatalysis due to the catalyzing treatment. This is because the initial deposition potential may promote nucleation and crystal growth, which determine the structural and magnetic properties of deposits. More detailed investigation of electrocatalysis of the substrate electrode requires solution of the problem as to why the properties of deposits with thickness of micrometer order are influenced by the substrate.

Electrical deposition of cobalt

Properties of deposits: Magnetic properties of electrically deposited Co (-2.5 μm thick) on Ni-based amorphous ribbon and Cu polycrystalline sheet are shown *versus* current density of the deposition in Fig. 5. It is believed that these magnetic properties are those of only the deposit layer because of the non-magnetic substrate for Ni-based ribbon and the para-magnetic substrate for Cu sheet, whose magnetization was easily separable from the component for deposit layer in the measurements. Coercive force (H_c) increased with an increase in current density of deposition. On the other hand, for Cu substrate, a larger remanent magnetization (M_r/M_s) was obtained at lower current density (decreased by up to half). This tendency of M_r/M_s was prominent for Ni-based amorphous substrate. These properties of deposits were dependent not only on current density but also on the species of substrates. There is a possibility that the composition of substrate is one of the factors controlling the magnetic properties of deposits. The magnetic properties of deposits on Fe-based and Co-based amorphous ribbons were difficult to separate from those of the bilayer materials, because of ferromagnetic substrates.

Fig. 6(a) and (b) show surface SEM images of deposits at a current density of 50 mA/cm^2. The shape and size of the needle like formations were dependent on species of substrate. The surface morphology of deposits on other amorphous substrate was different owing to alloying elements of the amorphous substrate.

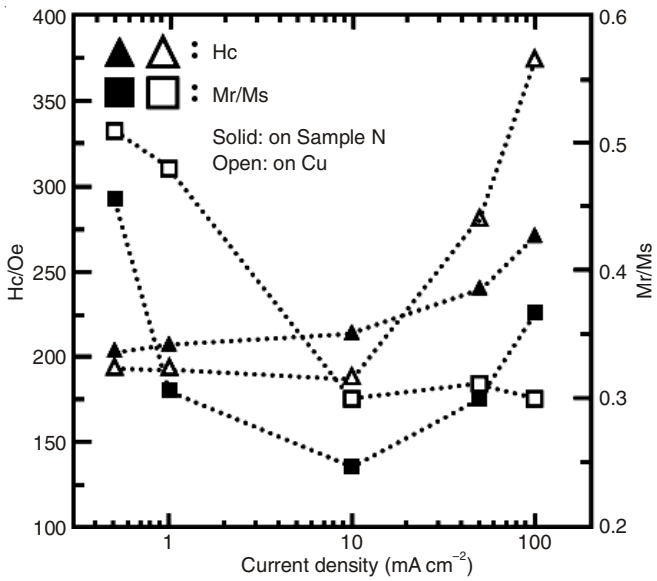

Fig. 5. Magnetic properties of electrodeposited Co films on amorphous NiSiB (N) ribbon and polycrystalline Cu sheet

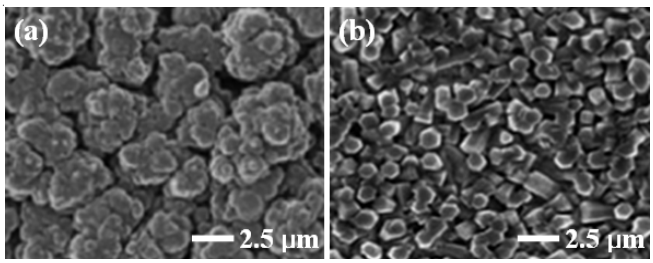

Fig. 6. (a) SEM surface images of electrically deposited Co films on amorphous NiSiB (N) ribbon and (b) polycrystalline Cu sheet, at a current density of 50 mA/cm^2

Each XRD profile of the deposits on several substrates presented 5 peaks of hcp Co. The degree of preferred orientation estimated by XRD profiles *versus* the current density is shown in Fig. 7. For Ni-based amorphous substrate, as shown in Fig. 7(a), the crystal face of deposit had a preferred orientation of (002). This preferred orientation of (002) and other orientations within 20 %, changed with current density. A similar tendency was obtained for other substrates, but the degree of preferred orientation and its dependence on current density differed with the species of substrate. On the other hand, Fig. 7(b) shows the results for polycrystalline Cu substrate. The degree of preferred orientation of faces other than (002) of this substrate was larger than the degree graph of other amorphous substrates at almost all current densities. In Fig. 7(c), the preferred orientations of (002) *versus* the current density for four kinds of substrates are shown. For amorphous substrates, there was a slight correlation of composition of substrates with the preferred orientation. The result for copper substrate was significantly different from amorphous substrates, which was large only at 10 mA/cm^2. This behaviour means that there is a possibility of an electrodeposition reaction controlled by not only the underlayer composition but also by its crystallinity.

Electrochemical deposition behaviour: We have experimentally confirmed the structural and magnetic properties of Co deposits dependancy not only on the current density but also on species of underlayer. Pangarov's theory on two-dimensional nucleation and crystal growth explains that the preferred orientation of deposit is determined by the over potential of electrodeposition [10]. Our idea is that the over potential may be affected by immersion potential of the substrate in the initial step of deposition. The over potential of the initial step is easily estimated by cathodic i-E curve of the substrate used as a working electrode.

The cathodic i-E curves for electrodes of four kinds of substrates are shown in Fig. 8(a). For each electrode, measurement was carried out from the immersion potential to the potential at a current density of 150 mA/cm^2. The other i-E curve is for a Co electrode electrodeposited on a Cu substrate.

The same curves (data not shown) were obtained for Co electrodes deposited on other substrates. The over potential (ç) of the electrodeposition is usually defined as follows:

$$\eta = E_{dep} - E_{rev} \quad (1)$$

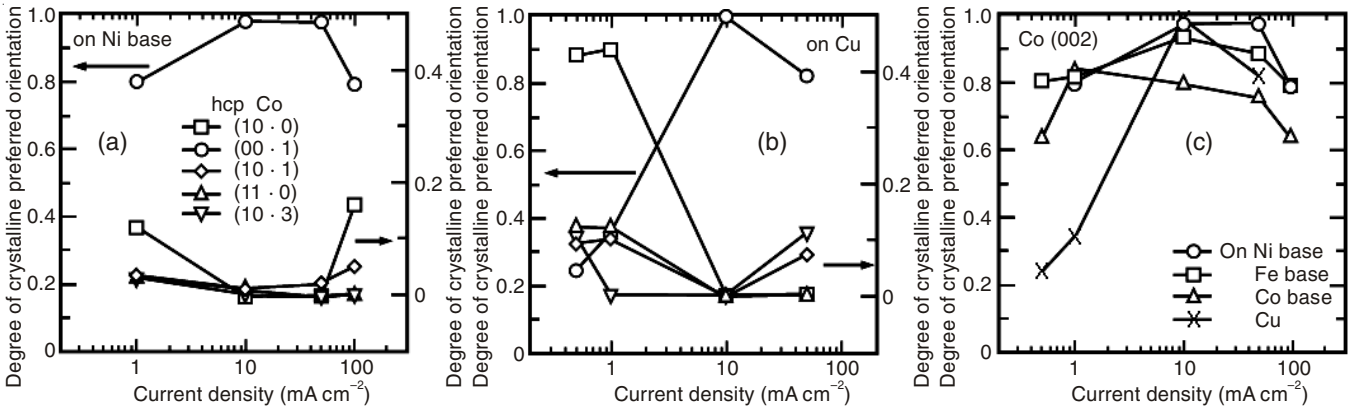

Fig. 7. Degree of preferred orientation (defined in the text) of XRD profiles for the electrically deposited Co films on (a) amorphous NiSiB (N) ribbon and (b) polycrystalline Cu sheet. (c) Only the data of hcp Co(002) for the films on respective substrates

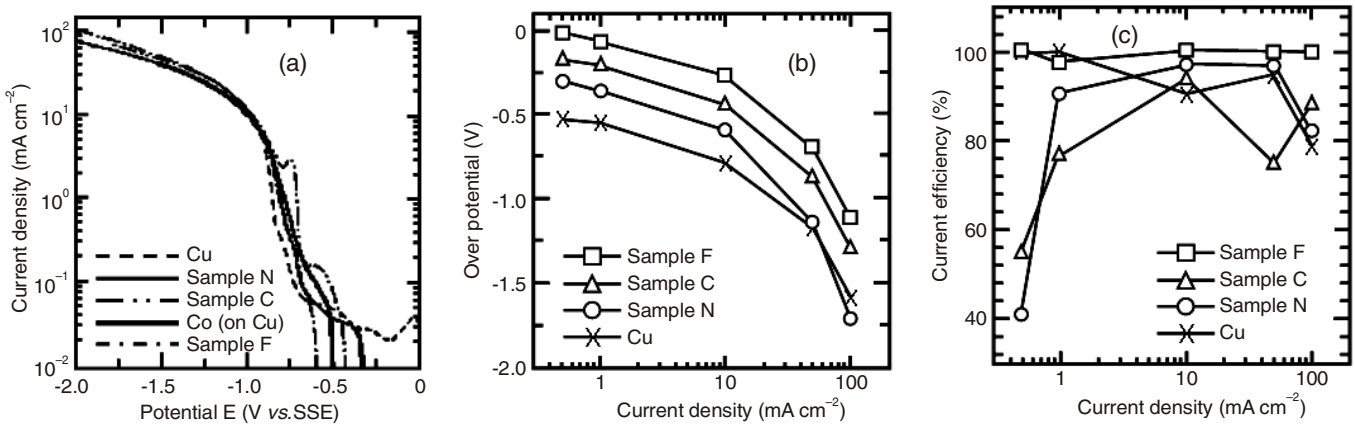

Fig. 8. (a) Cathodic polarization curves of respective amorphous ribbon electrodes, Cu sheet and electrodeposited Co on Cu sheet. (b) and (c) Over potential and current efficiency of electrodeposition of Co for these electrodes *versus* current density, respectively

where, E_{rev} is reversible potential and E_{dep} is electrode potential during deposition. For instance, E_{rev} is usually the equilibrium potential of a Co electrode for $Co^{2+} + e \longleftrightarrow Co$. It is supposed that for the same equilibrium reaction, E_{rev} gives immersion potential of the substrate used. However, in the case of deposition of some other element on a substrate, E_{rev} of the substrate is not equal to that of the deposit surface. We imagine that the over potential of the initial step is determined by E_{rev} of the substrate, which is dependent on alloying element of the substrate. Fig. 8(b) shows this over potential *versus* current density for respective substrates. It is natural that the reversible potential during electrodeposition is that of the deposit surface on which, influence of the immersion potential of the substrate is negligible, after the substrate is covered with one atomic layer of deposit. However, we believe that this over potential in the initial step of deposition is related to structural and magnetic properties of deposit through nucleation and crystal growth. Indeed, for an amorphous substrate, the order of preferred orientation of Co(002) deposited, as shown in Fig. 7(c), may be related to the order of over potential of the substrate electrode. Also, the difference of surface morphology of deposits depending on the species of substrates is related to the influence of species of substrates on the deposition behaviour on the surface of thick deposit [3]. It was reported that a hydrogen reaction occurred with electrodeposition, which was affected by the over potential of deposition [5]. The structural and magnetic properties of the deposit are influenced by hydrogen absorbed into the deposit. The current efficiency of Co electrodeposition is shown in Fig. 8(c) for several substrates. The current efficiency for Fe-based substrate was 100 % over the whole range of current density and for Ni-based and Co-based substrates, it was 40 to 50 % at lower current density. The current efficiency was significantly different depending on the species of substrates, which may be explained by the different deposition in the initial step for different species of substrates. Therefore, it is believed that this initial electrochemical deposition behaviour is one of the factors affecting formation of deposit. Copper substrate exhibited the most common result of current efficiency, which gives a high level at low current density and decreases with increasing current density due to hydrogen reaction. In the case of electrodeposition of Co on Fe-based substrate, a significantly high current density may be obtained because of not only over potential of deposition but also other factors (*e.g.*, adsorption of ions in the solution). This is an interesting phenomenon from fundamental and technological viewpoints, which is applicable to the restraint of hydrogen reaction. This study is focussed on the relationship between structural and magnetic properties of electrically deposited Co on amorphous alloy and Cu substrates and the electrochemical cathodic reaction dependent on the substrate. The properties of the deposit are found to be related to different over potentials of deposition, depending on composition of the substrate.

Conclusion

It is found that the structural and magnetic properties of non-electrically deposited films are determined by initial step of electrochemical parameters dependent on the species of substrate. This is because the nucleation and crystal growth are related to electrocatalysis of the substrate electrode for anodic oxidation of the reductant in non-electric deposition and the over potential of electrodeposition, whose parameters are dependent on the alloy element of substrate. The properties of both non-electrically deposited and electrically deposited films of a few micrometers thick are influenced by the initial behaviour of electrolytic deposition.

ACKNOWLEDGEMENTS

This research was supported by the Ministry of Trade, Industry and energy (MOTIE), KOREA, through the Education Support program for Creative and Industrial Convergence.

REFERENCES

1. Y. Lin, J.W. Shaffer and H.A. Sodano, *Smart Mater. Struct.*, **19**, 124004 (2010).
2. D.-Y. Lin, Y. Jiang and X.-X. Wang, *Adv. Eng. Mater.*, **12**, B70 (2010).
3. R. Rastogi and A. Pandey, *J. Chem. Technol.*, **17**, 381 (2010).
4. K. Wykpis, A. Budniok and E. Lagiewka, *Mater. Sci. Forum*, **636-637**, 1053 (2010).
5. A.P. Abbott, J.C. Barron and K.S. Ryder, *Inst. Metal Finish*, **87**, 201 (2009).
6. Y. Wang, Z. Jiang, X. Liu and Z. Yao, *Appl. Surf. Sci.*, **255**, 8836 (2009).
7. C.S. Han, C.H. Chun and S.O. Han, *Kor. J. Mater. Res.*, **19**, 319 (2009).
8. C. Borioli, S. Franz, P.L. Cavallotti, M. Cantoni and R. Bertacco, *J. Electrochem. Soc.*, **157**, D437 (2010).
9. P.L. Cavallotti, B. Bozzini and G. Zangari, Progress of Electrocatalysis: Theory and Practice p. 1787 (1994).
10. N.A. Pangarov and S.D. Volmer, *Electrochim. Acta*, **7**, 139 (1962).